Electronic structure of zincblende ZnSe: theory and experiment

1994 J. Phys.: Condens. Matter 6 3207

(http://iopscience.iop.org/0953-8984/6/17/010)

J. Phys.: Condens. Matter 6 (1994) 3207–3219. Printed in the UK

Electronic structure of zincblende ZnSe: theory and experiment

R Markowski, M Piacentini‡, D Debowska†, M Zimnal-Starnawska†, F Lama§, N Zema‖ and A Kisiel†

† Institut Fizyki, Uniwersytet Jagiellonski, ulica Reymonta 4, 30-059 Krakow, Poland

‡ Dipartimento di Energetica, Università di Roma 'La Sapienza', Via A Scarpa 14, 00161 Rome, Italy

§ Consorzio INFM, Via Dodecaneso 33, 16146 Genova, Italy

‖ Istituto di Struttura della Materia, Consiglio Nazionale delle Ricerche, Via E Fermi 38, 00044 Frascati, Italy

Received 20 September 1993, in final form 22 December 1993

Abstract. In this paper we present a comprehensive study of the tetrahedral semiconductor ZnSe crystallizing in the zincblende structure. The electronic structure of ZnSe has been determined first using the *ab initio* self-consistent linear muffin-tin orbital method with a local-density form of the exchange–correlation functional. Then it has been adjusted to reproduce the experimental energy positions of the Zn 3d bands and of the optical gap. The adjusted electronic structure, densities of states and interband optical properties are presented and compared with previous calculations. Good agreement with experimental photoemission and bremsstrahlung isochromat measurements was found after including an energy-dependent lifetime broadening. We measured the reflectivity of ZnSe with high resolution from 4 to 30 eV and the high-energy region of the spectra has been interpreted on the basis of the present calculation.

1. Introduction

A strong interest exists in the electronic properties of II–VI semiconductors because of their important applications, e.g. in the construction of heterostructures and other low-dimensional systems, as non-linear optical devices and as host crystals for semimagnetic semiconductors. This paper, which is meant to precede a detailed study of the reflectivities of several ternary compounds obtained by alloying ZnSe with a transition metal of the first row, presents a comprehensive study, both theoretical and experimental, of pure ZnSe.

The energy bands of ZnSe have been calculated by several workers using either semiempirical methods [1–8] or self-consistent methods [9–13]. We started to perform an *ab initio* self-consistent ground-state energy band calculation of ZnSe using the lattice constant as the only experimental input to the numerical procedure. After obtaining the band structure, we adjusted the energy bands by varying the potential parameters in order to reproduce the positions of the Zn 3d bands derived from photoemission measurements and by shifting the conduction bands to higher energies in order to reproduce the fundamental optical gap. The theoretical density of states was calculated for the valence bands and for the conduction bands up to 30 eV above the valence band maximum and compared with photoemission [8, 14–16] and bremsstrahlung isochromat spectra [8]. The calculated energies and wavefunctions were used to determine the optical properties of the material.

The reflectivity of ZnSe has been measured by several workers in the visible and near-ultraviolet regions [17, 18]. Petroff and co-workers [2, 3] measured the reflectivity of ZnSe

0953-8984/94/173207+13$19.50

at low temperatures up to 11 eV and gave a thorough interpretation of the valence-to-conduction band spectra, based on empirical pseudopotential band-structure calculations. Using synchrotron radiation, Freeouf [19] extended the reflectivity measurements to about 23 eV, finding new broad features assigned to transitions from the Zn 3d states. We measured the reflectivity of ZnSe single crystals at room temperature (RT) and at liquid-nitrogen temperature (LNT) over a broad energy range with high resolution. In the low-energy region our spectra are similar to those already published, but a wealth of sharp fine structures has been found between 11 and 13.5 eV. The experimental spectra are discussed on the basis of the calculated band structure and compared with the theoretical spectra.

2. Experiment

The reflectivity measurements were performed at the vacuum ultraviolet beam line of the PULS laboratories at INFN Frascati National Laboratories. Synchrotron radiation from the Adone storage ring was focused onto the entrance slit of a 1 m near-normal-incidence monochromator equipped with two gratings interchangeable under vacuum conditions. A 1440 lines mm^{-1} gold-coated grating was used in the 10–30 eV photon energy range and a 600 lines mm^{-1} Al+MgF_2-coated grating was used to cover the 4–12 eV photon energy range. The average resolution $\Delta E/E$ used for these measurements was better than 1×10^{-3} over the entire spectral range.

A ZnSe single crystal was cleaved before being mounted inside the reflectometer from an ingot grown by the Bridgman method. The sample was attached to the cold finger of a LNT cryostat. The reflected beam was collected either with a Bendix electron multiplier M306 in the 10–30 eV range or with a solar blind photomultiplier equipped with a LiF window in the 4–10 eV range. Data acquisition was done by means of a lock-in amplifier whose output was digitized and fed into the set-up control computer.

3. Method of calculation

The calculation of the optical properties of zinc selenide involved the following steps:

(a) self-consistent calculations of the band structure E_n^k;

(b) adjustment procedure for reproducing the positions of the semicore Zn 3d bands and the experimental value of the fundamental optical gap;

(c) calculation of the partial densities $D_l(\omega)$ of states;

(d) calculation of the dipole transition matrix elements M_{fi}^k;

(e) calculations of the dielectric function $\epsilon(\omega)$ and reflectivity $R(\omega)$.

The band structure of ZnSe was obtained using the self-consistent linear muffin-tin orbital (LMTO) method [20]. All relativistic corrections, namely the mass velocity, the Darwin shift and the spin–orbit coupling, as well as the 'combined correction term' [21] were included in the calculation. ZnSe crystallizes in the tetrahedral environment as either zincblende of wurtzite structure. In our calculation we considered the zincblende structure (space group T_d^2), with the two atoms Zn and Se at the positions (0, 0, 0) and $(\frac{1}{4}, \frac{1}{4}, \frac{1}{4})$, respectively, and two empty spheres [22] at the positions $(\frac{1}{2}, \frac{1}{2}, \frac{1}{2})$ and $(\frac{3}{4}, \frac{3}{4}, \frac{3}{4})$. The experimental lattice constant of 5.668 Å was applied throughout the calculation. The exchange–correlation local density (LD) potential was used in the form proposed by Vosko *et al* [23]. All the calculations were carried out in a single energy panel, using 4s, 4p

and 3d basis functions for Zn and 4s, 4p and 4d functions for Se. The computed binding energies of the Zn 3d levels in the self-consistent ground-state band structure are too small (average value: 6.35 eV) and in disagreement with respect to the value of 9.2 eV obtained by photoemission measurements [14, 24]. The discrepancy between the calculated and observed binding energies of the semicore Zn 3d states is a correlation effect which is mainly the result of changing the occupancy of Zn 3d levels in the excitation process. The experimental value of the binding energies of these states was reproduced by changing the potential parameters in the last step of the LMTO procedure. The band structure calculated with this method is presented in figure 1. The topmost valence band Γ_{15} is split owing to spin–orbit coupling into a fourfold state Γ_8 and a twofold state Γ_7 ($\Delta_0 = 0.45$ eV). The total number of bands is equal to 36, the first nine of them being situated below the Fermi level. Figure 2 shows a schematic layout of the self-consistent bands of ZnSe, deduced from the potential-parameter-related quantities V_l, B_l, C_l and A_l that specify the square-well pseudopotential, the bottom, the mass centre and the top of the l band, respectively [21].

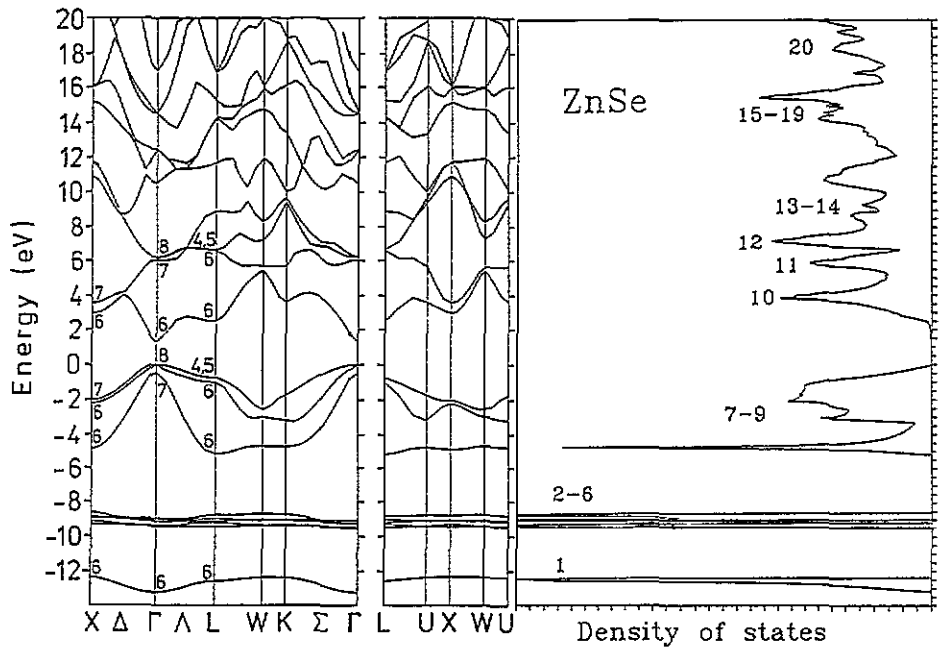

Figure 1. Band structure of zinc selenide. The energy zero is taken to be the top of the valence band. On the right-hand side we show the total density of states. The numbers near the main peaks denote the serial numbers of the bands.

In table 1 and table 2 we summarize the eigenvalues of several valence and conduction states at selected high-symmetry points and compare them with the results of other calculations and with the experimental determinations.

Once the band structure had been obtained, the total density of states was calculated and is presented in figure 1. We have also obtained the partial densities of states on each site and the main results are given in figure 3. We have used 12 divisions for ΓX and an

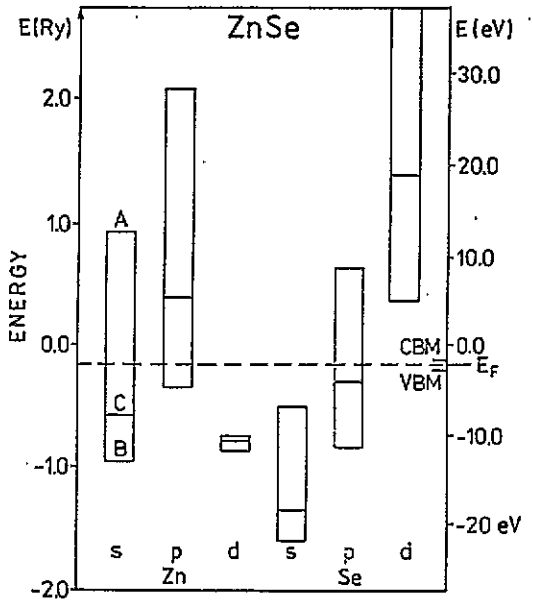

Figure 2. Schematic layout of the electronic structure of ZnSe. The bars depict the extent of the n, l bands as defined by the parameters A (top of the band), C (band centre) and B (bottom of the band). The valence band maximum (VBM) and the conduction-band minimum (CBM) are also marked.

energy step as small as 0.045 eV. The zero of the energy scales in figures 1 and 3 is at the top of the valence bands.

Within the one-electron picture and in the limit of vanishing linewidth, the frequency-dependent imaginary part of the dielectric function $\epsilon(\omega)$ due to interband transitions is given by the standard formula [7]

$$\epsilon_2(\omega) = \frac{4\pi^2 e^2}{3m^2\omega^2} \sum_i \sum_f \int_{BZ} \frac{2}{(2\pi)^3} d^3k \, |M_{fi}^k|^2 \delta(E_f^k - E_i^k - \hbar\omega) \tag{1}$$

where E_i^k and E_f^k are the energies of the occupied and empty states, respectively, at a given k-vector. So, the imaginary part of the dielectric function for transitions between band states i and f can be expressed in terms of an integral containing the dipole matrix elements and an energy-conserving delta function. The computation of the wavevector-dependent momentum matrix element

$$M_{fi}^k = \langle fk | \frac{\hbar\nabla}{i} | ik \rangle$$

becomes rather straightforward in the case of LMTO since the intersite transitions do not exist because of the nature of the orbitals [27].

The integration of equation (1) over k-space was performed by the tetrahedron method [28] based on 240 k-points in the irreducible part (one forty-eighth) of the Brillouin zone. The imaginary part of the dielectric function was calculated for photon energies ranging up to 30 eV. The real part of the dielectric function was obtained by the Kramers–Kronig transformation of the computed $\epsilon_2(\omega)$, to which we attached a tail function of the

Table 1. Calculated and experimental eigenvalues for zinc selenide valence bands at the high-symmetry points Γ, X and L. All energies are referred to the top of the valence bands. Column (1), present VLMTO calculation with spin–orbit coupling (the Zn 3d enegy is the average value); column (2), experimental values; column (3), EPM calculation with spin–orbit coupling [7]; column (4), LCGO calculation without spin–orbit coupling [10]; column (5), EPM calculation without spin–orbit coupling [8]; column (6), MOPW calculation without spin–orbit coupling [25].

	(1)	(2)	(3)	(4)	(5)	(6)
Γ_6^v (eV)	−13.18	−15.2[a]	−12.25	−12.67	−12.13	−12.9
Γ_7^v (eV)	−0.45		−0.45	—	—	—
Γ_8^v (eV)	0.00	0.00	0.00	0.00	0.00	0.00
Zn 3d (eV)	−9.20	−9.2[a]	—	−6.70	—	—
Δ_0 (eV)	0.45	0.43[b]	0.45	—	—	—
X_6^v (eV)	−12.32	−12.5[a]	−10.72	−11.55	−10.61	−12.4
X_6^v (eV)	−4.90	−5.6[a]	−4.96	−4.69	−4.86	−3.20
X_6^v (eV)	−2.24		−2.17	−2.16	−1.96	−1.20
X_7^v (eV)	−2.06	−2.1[a]	−1.96	—	−1.96	—
L_6^v (eV)	−12.53	−13.1[a]	−11.08	−11.83	−10.97	−12.60
L_6^v (eV)	−5.19	−5.6[a]	−5.08	−5.15	−4.98	−3.40
L_6^v (eV)	−1.03		−1.04	−0.85	−0.78	−0.50
$L_{4,5}^v$ (eV)	−0.75	−1.3[a]	−0.76	—	−0.78	—
		−0.7[c]				
Δ_1 (eV)	0.28	0.25[d]	0.30	—	—	—

[a] From [14]
[b] From [17].
[c] From [15].
[d] Present work.

form $\epsilon_2(\omega) = \beta\omega/(\omega^2 + \gamma^2)^2$ for energies greater than 30 eV. We chose $\gamma = 4.5$ eV, whereas β was determined by the continuity of ϵ_2 at 30 eV. Knowledge of the complex dielectric function $\epsilon(\omega) = \epsilon_1(\omega) + i\epsilon_2(\omega)$ allowed for the computation of the theoretical reflectivity spectrum $R(\omega)$ [7].

It is known that the LMTO method cannot reliably describe bands positioned higher than 1–2 Ryd above the average interstitial potential [20]. Although in our calculation we limited the energy range to 30 eV above the valence band maximum, we should not expect good coincidence between theory and experiment for energies higher than 20 eV. The contribution to the imaginary part of the dielectric function arising from transitions originating in the upper part of the valence bands to the higher conduction bands is more uncertain than the other contributions. The quantitative comparison of the theoretical reflectivity spectrum with the experimental spectrum is only meaningful if the matrix elements of **P**, the momentum operator, are included in the calculation. The evaluation of the matrix elements in the multi-panel procedure is a very complicated problem from the mathematical point of view. On the other hand we should not expect much better results in such a sophisticated calculation performed in the one-electron approximation. This is the reason why the whole calculations were performed in a single energy panel.

4. Results and discussion

The lowest band of the occupied valence states is mainly s like and is localized on an anion. The valence band maximum has Se 4p character. The Zn 3d bands fall in the middle of

Table 2. Calculated and experimental eigenvalues for zinc selenide conduction bands at the high-symmetry points Γ, X and L. All the energies are referred to the bottom of the conduction bands. Column (1), present VLMTO calculation with spin–orbit coupling; column (2), experimental values; column (3), EPM calculation with spin–orbit coupling [7]; column (4), LCGO calculation without spin–orbit coupling [10]; column (5), EPM calculation without spin–orbit coupling [8]; column (6), MOPW calculation without spin–orbit coupling [25]; $E_g^{(1)}$ calculated with spin–orbit coupling; $E_g^{(2)}$, calculated without spin–orbit coupling.

	(1)	(2)	(3)	(4)	(5)	(6)
Γ_6^c (eV)	0.00	0.00	0.00	0.00	0.00	0.00
Γ_7^c (eV)	4.81	4.39[a]	4.57	4.60	5.00	5.60
Γ_8^c (eV)	4.97	4.56[a]	4.66	—	5.00	—
X_6^c (eV)	1.69	—	1.76	1.85	1.71	2.50
X_6^c (eV)	2.30	—	2.41	2.41	1.96	2.60
L_6^c (eV)	1.25	1.4[a]	1.20	1.08	1.19	1.60
L_6^c (eV)	5.34	—	4.92	4.87	4.91	6.00
L_{45}^c (eV)	5.42	—	4.96	—	4.91	6.70
$E_g^{(1)}$ (eV)	1.22	2.82[b]	2.76	—	—	—
$E_g^{(2)}$ (eV)	1.13	—	—	—	2.89	3.00

[a] Values extracted from our experimental determinations, photoemission determinations [15] and E_g determination [16].
[b] From [26], measured at 10 K.

the sp valence band manifold. Zinc selenide is a direct Γ_8^v–Γ_6^c gap semiconductor. The calculated values of the spin–orbit splittings of the highest valence band at the Γ point, namely $\Delta_0 \equiv \Gamma_7^v - \Gamma_8^v = 0.45$ eV, and at the L point, namely $\Delta_1 \equiv L_6^v - L_{45}^v = 0.28$ eV, are in excellent agreement with experiment (table 1). The average theoretical separation of the Zn $3d_{5/2}$–$3d_{3/2}$ levels is equal to 0.36 eV, which agrees well with the spin–orbit splitting of these states of the free ion [29]. In zinc compounds it has been difficult to observe the experimental, well defined value of the splitting.

As has already been discussed elsewhere [10], the mass-velocity and Darwin relativistic corrections, when included in the calculation, tend to worsen the agreement between the theoretical and experimental band gaps. In fact, the direct band gap of ZnSe was decreased by 0.31 eV with respect to the non-relativistic result after inclusion of the two scalar relativistic corrections. The spin–orbit coupling introduced into the numerical procedure as a formal perturbation term in the Hamiltonian increased the value of the fundamental band gap by 0.4 eV. It finally results in an increase in the fundamental energy gap.

The LD approximation is known to fail in predicting the energy band eigenvalues in semiconductors owing to the difficulty of including correctly many-body electron correlation and exchange interactions. The difference between the theoretical eigenvalues and the experimental excitation energies is characterized by the self-energy [16, 30]. The self-energy correction of the conduction bands of several IV and III–V semiconductors is nominally independent of energy [16]. For this reason, it has become common practice to shift rigidly all the conduction bands to higher energies in order to reproduce the experimental band gap [11, 13, 31]. With this procedure, good agreement between the calculated conduction band density of states and bremsstrahlung isochromat spectra or between the calculated $\epsilon_2(\omega)$ and the experimental spectrum can be achieved.

In figure 4 we compare the calculated density of states of ZnSe with selected experimental photoemission spectra [8, 14, 15] and a bremsstrahlung isochromat spectrum [8]. The

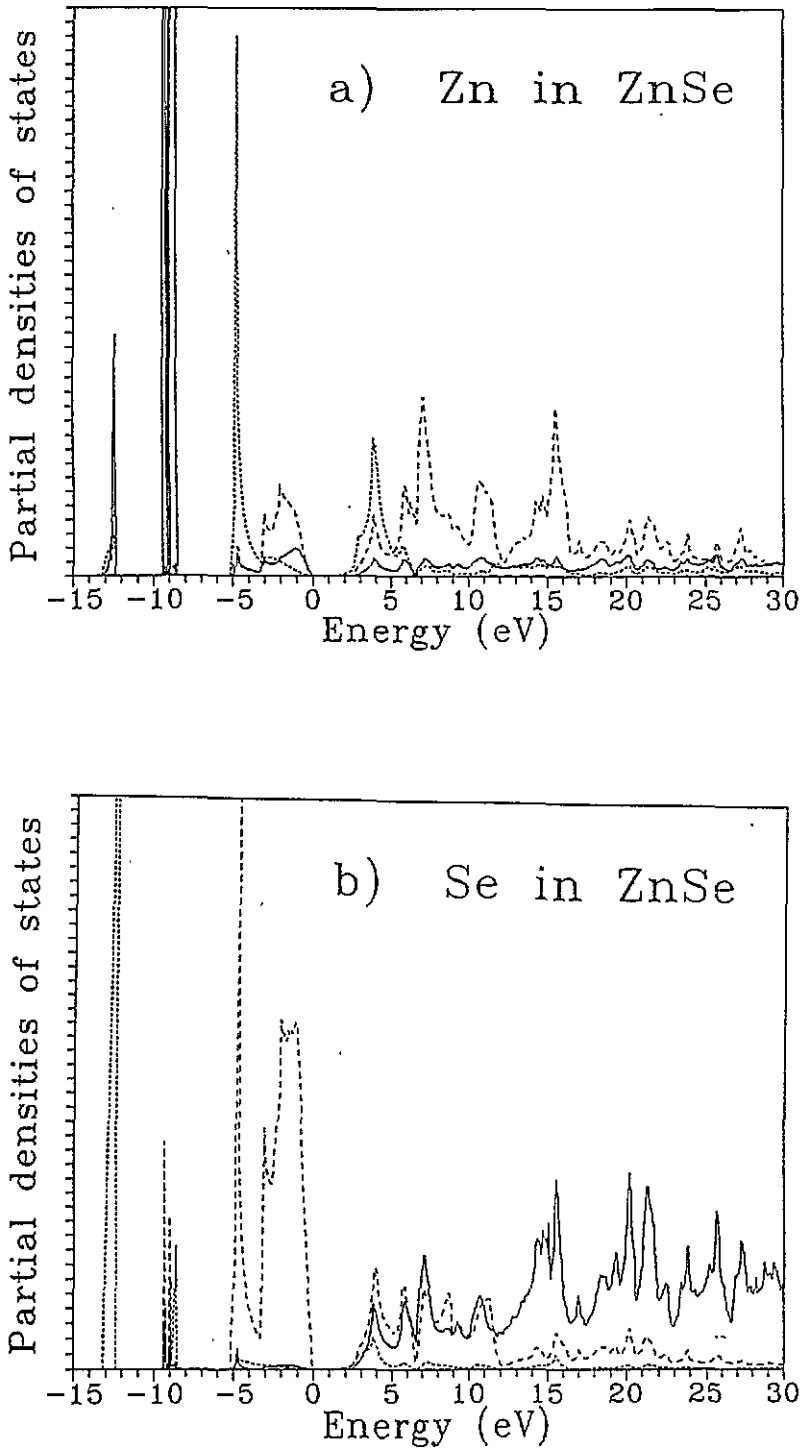

Figure 3. (a) Partial densities of states at a Zn site. (b) Partial densities of states at a Se site: ----, s-like states; – – –, p-like states; ——, d-like states.

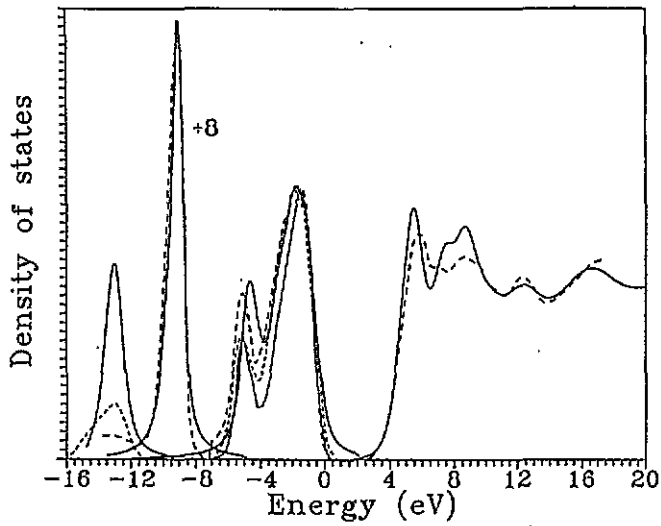

Figure 4. Calculated density of states of ZnSe (——) after empirical self-energy corrections, lifetime and experimental resolution broadening, compared with the photoemission and bremsstrahlung isochromat spectra: ----, x-ray photoelectron spectrum after [14]; ·····, ultraviolet photoelectron spectrum after [15], shifted to lower energies by 0.2 eV for better agreement [32]; – – –, x-ray photoelectron and bremsstrahlung isochromat spectra from [8], the x-ray photoelectron spectrum has been shifted to lower energies by 0.6 eV for better agreement with theory and the other experimental spectra [32].

calculated conduction band density of states has been shifted by 1.5 eV to higher energies in order to match the fundamental gap. Then it has been convoluted with a Lorentzian function to include lifetime broadening and with a Gaussian function to take into account the experimental resolution. The lifetime of conduction electrons is energy dependent. Inelastic electron–electron scattering is the main decay process when the electron energy exceeds the value that is approximately twice the fundamental band gap [16, 33]. In this case the lifetime decreases almost linearly in a broad energy range [16]. Near the bottom of the conduction band the lifetime is caused mainly by the phonon production and can be considered almost constant [16]. Figure 4 shows very good correspondence between both the energy positions and the intensities of the structures in the calculated conduction band density of states and the bremsstrahlung isochromat spectrum [8]. For the filled states we corrected the positions of the semicore Zn 3d states as mentioned before and also used the energy-dependent broadening. With this procedure we obained good agreement between theoretical and experimental valence band densities of states. The energies of the density-of-states maxima associated with the seventh band and with the first band (Se 4s) are shifted about 0.5 eV with respect to the experimental values, since we did not include the real part of the self-energy correction [11, 16] in our numerical procedure.

Figure 5 shows the reflectivity spectra of ZnSe measured between 4 and 30 eV at RT and between 4 and 20 eV at LNT. The experimental reflectivities are compared also with the calculated value. The measured spectra are similar to those measured by Freeouf [19], but ours show better resolution in the high-energy region, where several new structures appeared between 11 and 13.5 eV as shoulders in the RT spectrum, and as well resolved peaks in the LNT spectrum. Good agreement was also found with the reflectivity spectrum measured by Petroff *et al* [2, 3] between 4 and 10 eV.

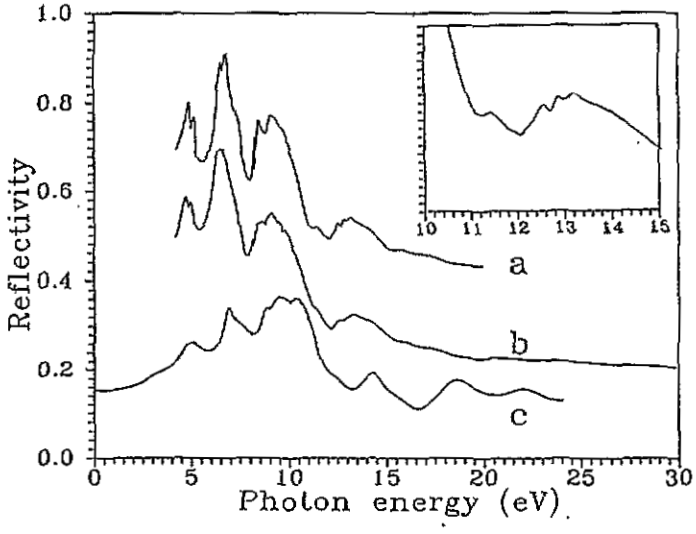

Figure 5. Reflectivity spectra of ZnSe measured at LNT (curve a) and at RT (curve b), compared with the theoretical spectrum (curve c). Curves a and b have been displaced upwards by 0.4 and 0.2, respectively, to avoid overlapping. The inset shows the region of the core transitions measured at LNT on an expanded scale.

From the reflectivity spectra we derived the other optical constants of ZnSe by means of the Kramers–Kronig transformations, completing our spectra below 4 eV with the reflectivity spectrum measured by Cardona [17] and using an exponential tail at high energies. In table 3 we list the calculated and experimental positions of the main structures in the ϵ_2 and reflectivity spectra.

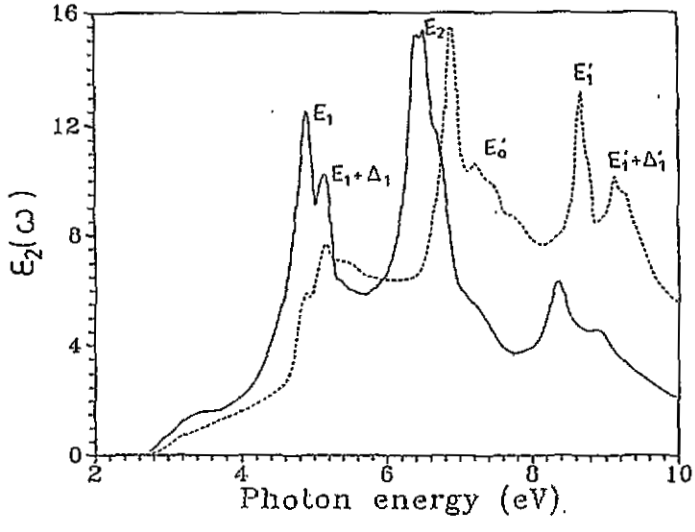

Figure 6. Imaginary part of the dielectric function for ZnSe between 2 and 10 eV: ——, LNT ϵ_2 spectrum, obtained from the Kramers–Kronig transformations of the reflectivity; ·····, theoretical ϵ_2 spectrum.

Table 3. Calculated and experimental values (at LNT) of energy gaps in zinc selenide compared with other theoretical calculations and experimental spectra. Column (1), calculated ϵ_2 spectrum (present work); column (2), LNT experimental ϵ_2 spectrum (present work); column (3), LNT reflectivity spectrum (present work); column (4), reflectivity spectrum [3]; column (5), LNT reflectivity spectrum [19]; column (6), theoretical EPM calculation with spin–orbit coupling [7]; column (7), theoretical LCGO calculation without spin–orbit coupling [11]; column (8), theoretical OLCAO calculation without spin–orbit coupling [13].

	(1)	(2)	(3)	(4)	(5)	(6)	(7)	(8)
E_0 (eV)	2.80[a]				2.663[b]	2.82	1.83	1.65
E_1 (eV)	4.91	4.915	4.88	4.75	4.9	4.72	4.02	3.8
$E_1 + \Delta_1$ (eV)	5.16	5.16	5.13	5.05	5.2	5.00		
				6.00		5.97	5.53	5.8
		6.39	6.40			6.20	5.86	
E_2 (eV)	6.90	6.525	6.54	6.50	6.55	6.47		
	7.23	6.70	6.81	6.63	6.8	6.62		
E_0' (eV)	7.47	7.21	7.24	7.15	7.3	7.10	6.14	
	7.74	7.38	7.45	7.60		7.42	7.08	
				7.80		7.88		
E_1' (eV)	8.67	8.35	8.40	8.46	8.4	8.50	7.53	7.8
	9.12	8.92	9.06	8.97	9.2	8.85		
					9.7			
	11.6	11.37	11.40		11.35			
	12.1	11.92	11.98					
		12.2	12.2					
		12.51	12.55		12.5			
		12.84	12.87					
		13.1	13.20		13.1			
	13.9		13.8					
	15.9	15.7	15.8		15.8			
	17.2	16.8	16.9					
	18.9	18.7	18.7					
	20.7		20.5[b]		20.5			
			21.6[b]					
	22.5		23.2[b]					
			25.0[b]					

[a] Value used to fit the energy gap.
[b] RT values.

In figure 6 we compare in the 2–10 eV region the theoretical spectrum of the imaginary part of the dielectric function with the experimental spectrum derived from the reflectivity measurements. The comparison between the two spectra shows very good agreement. This energy region has already been studied in detail by several workers [2, 3, 7, 11, 17, 18]. The assignment of the main structures is summarized below. The E_0 reflectivity maximum (not shown in figures 5 and 6) corresponds to the minimum energy gap at Γ. The E_1 and $E_1+\Delta_1$ structures arise from transitions along the Λ direction near the L point. The higher intensity of the experimental E_1 and $E_1 + \Delta_1$ structures with respect to the calculated structures has been attributed to the electron–hole interaction [34, 35]. Structure corresponding to the E_2 maximum arises from a large Brillouin zone region. The E_0' structure corresponds to transitions near Γ and along the Δ direction whereas E_1' originates in transitions near the L point.

At energies above 11 eV, the structures arise from transitions involving the Zn 3d and Se 4s states [19]. In this energy region the reflectance decreases sharply because the oscillator strength of transitions from the valence to the conduction band has been

nearly exhausted. Good agreement is obtained between the calculated ϵ_2 spectrum from the contribution given by the transitions originating in the Zn 3d and Se 4s states and the broad features of the experimental spectrum, as shown in figure 7. The first maximum of the calculated ϵ_2 contribution at about 14 eV fits the broad feature between 11 and 15 eV in the experimental spectrum well. This maximum derives from the large volume of the Brillouin zone around the L–W–K symmetry points, with the final states in the first conduction band. The experimental broad bands with maxima at 15.8, 16.9, 20.5 and 25 eV can be attributed to the corresponding maxima of the calculated spectrum with initial states in the Zn 3d bands. The weaker maxima at about 19 and 23 eV could be attributed to the contribution from the Se 4s bands.

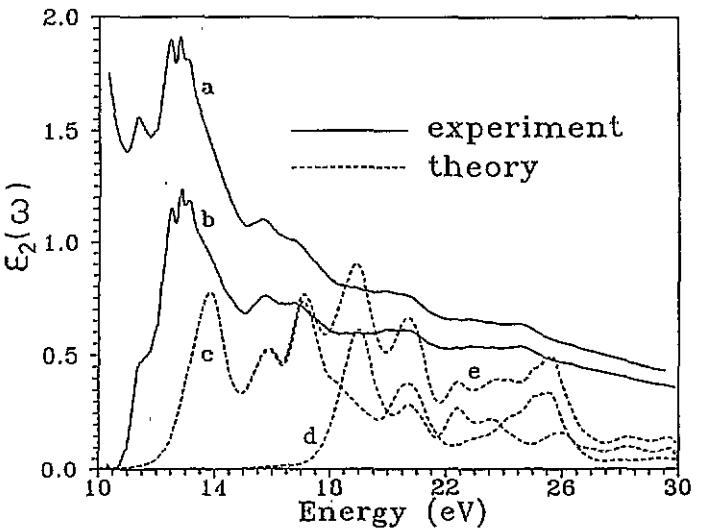

Figure 7. Imaginary part of the dielectric function for ZnSe between 10 and 30 eV: curve a, LNT experimental spectrum (the portion above 20 eV has been taken from the RT spectrum); curve b, LNT experimental spectrum after subtracting a smooth exponential background extrapolated from transitions from the valence to conduction band; curve c, theoretical contribution from the Zn 3d transitions; curve d, theoretical contribution from the Se 4s transitions; curve e, theoretical contribution from the superposition of the Zn 3d and Se 4s transitions.

The sharp features between 11.2 and 13.5 eV are not present in the contributions to the ϵ_2 spectrum from the Zn 3d states. The origin of these features could be attributed to transitions originating in the upper part of the valence band to the higher conduction bands. However, when lifetime broadening was included in the calculation, the sharp valence features above approximately 10 eV were almost entirely smoothed out. The absence of the peaks in the calculated one-electron spectrum, their significant narrowing as the temperature decreases from RT to LNT and their lower energy with respect to the calculated spectrum strongly suggest an excitonic origin. The energies of the maxima of these fine structures present in the ZnSe reflectivity spectrum are almost the same as the corresponding values in the ZnTe reflectance [36], indicating that they correspond to transitions well localized on the Zn site. M_0 thresholds are expected in the correspondence of the minima of the lowest conduction band, at the Γ, L and X points of the Brillouin zone. The lowest structure at 11.37 eV can be assigned to a core exciton at the Γ point, the structure at 11.92 eV being

its spin–orbit partner. The other maxima at 12.2, 12.51, 12.84 and 13.1 eV can be assigned to core excitons at the L point, where the degeneracy of the Zn 3d states is completely removed. The theory suggests that excitonic transitions at the X point contribute also to the two last maxima.

5. Conclusions

The interband optical properties of ZnSe have been investigated. We applied a first-principles LMTO method supported by a very simple procedure which aligns the experimental and theoretical energy scales. The calculation was performed in the scheme of the LD approximation. The comparison of our theoretical results with experiments reflects the influence of many-body effects. In general, our calculations performed in a state-of-the-art manner, i.e. with matrix elements and relativistic effects included, allow consistent assignment of structures in the experimental reflectivity spectrum and understanding of the physical mechanism of the transitions observed in the $R(\omega)$ and bremsstrahlung isochromat spectra.

Acknowledgments

We are grateful to P M Lee from Lancaster University for useful discussions. Financial support for the exchange visits was obtained through the Direct Research Exchange Programme between the University of Rome 'La Sapienza' and the Jagellonian University. This work was partially supported in the framework of project PB 931/2/91 supported in 1991–3 by the Polish State Committee for Scientific Research, and by the Italian Consorzio INFM and CNR through the GNSM.

References

[1] Cohen M L and Bergstresser T K 1966 *Phys. Rev.* **141** 789
[2] Petroff Y, Balkanski M, Walter J P and Cohen M L 1969 *Solid State Commun.* **7** 459
[3] Walter J P, Cohen M L, Petroff Y and Balkanski M 1970 *Phys. Rev.* B **1** 2661
[4] Chelikowski J, Chadi D J and Cohen M L 1973 *Phys. Rev.* B **8** 2786
[5] Chelikowski J and Cohen M L 1976 *Phys. Rev.* B **14** 556
[6] Vogl P, Hjalmarson H P and Dow J D 1983 *J. Phys. Chem. Solids* **44** 365
[7] Cohen M L and Chelikowsky J R 1988 *Electronic Structure and Optical Properties of Semiconductors (Springer Series in Solid State Sciences 75)* (Berlin: Springer) p 112
[8] Chelikowsky J R, Wagner T J, Weaver J H and Jin A 1989 *Phys. Rev.* B **40** 9644
[9] Stukel D, Euwema R, Collins T, Herman F and Kortum R 1969 *Phys. Rev.* **179** 740
[10] Wang C S and Klein B M 1981 *Phys. Rev.* B **24** 3393
[11] Wang C S and Klein B M 1981 *Phys. Rev.* B **24** 3417
[12] Bernard J E and Zunger A 1987 *Phys. Rev.* B **36** 3199
[13] Huang Ming-Zhu and Ching W Y 1993 *Phys. Rev.* B **47** 9449
[14] Ley L, Pollak R A, McFeely F R, Kowalczyk S P and Shirley D A 1974 *Phys. Rev.* B **9** 600
[15] Eastman D E, Grobman W D, Freeouf J L and Erbudak M 1974 *Phys. Rev.* B **9** 3473
[16] Jackson W B and Allen J W 1988 *Phys. Rev.* B **37** 4618
[17] Cardona M 1961 *J. Appl. Phys.* **32** 2151
[18] Ebina A, Yamamoto M and Takahashi T 1972 *Phys. Rev.* B **6** 3786
[19] Freeouf J L 1973 *Phys. Rev.* B **7** 3810
[20] Andersen O K 1975 *Phys. Rev.* B **12** 3060
[21] Skriver H L 1984 *The LMTO Method (Springer Series in Solid State Sciences 41)* (Berlin: Springer) p 95

[22] Jarlborg T and Freeman A J 1979 *Phys. Lett.* **74A** 399
[23] Vosko S H, Wilk L and Nusair M 1980 *Can. J. Phys.* **58** 1200
[24] Vesely C J and Langer B W 1971 *Phys. Rev.* B **4** 451
These workers give a binding energy of 10.39 eV below the centre of the energy gap, i.e. 9.0 eV with respect to the top of the valence bands.
[25] Kurganski S I, Farberovich O W and Domashevska E P 1980 *Phys. Tech. of Semiconduct.* **14** 1315
[26] Theis D 1977 *Phys. Status Solidi* b **79** 125
[27] Koenig C and Khan M A 1983 *Phys. Rev.* B **27** 6129
[28] Lehman G and Taut M 1972 *Phys. Status Solidi* b **54** 469
[29] Moore C E 1958 *Atomic Energy Levels (NBS Circular No. 467)* (Washington, DC: US Department of Commerce)
[30] Perdew J P and Zunger A 1981 *Phys. Rev.* B **23** 5084
[31] Markowski R and Podgorny M 1991 *J. Phys.: Condens. Matter* **3** 9041
[32] Usually the leading edge of the valence band photoemission spectrum is extrapolated with a straight line, the zero crossing of which is taken as the 'top' of the valence bands. This method is somewhat arbitrary. Jackson and Allen [16] have shown that, in the case of Ge, some disagreement in the binding energies of valence band peaks between different spectra from the literature could be taken care of by shifting the spectra properly. For this reason we feel justified to have followed the same procedure also for ZnSe.
[33] Kane E O 1967 *Phys. Rev.* **159** 159
[34] Matatagui E, Thompson A G and Cardona M 1968 *Phys. Rev.* **176** 950
[35] Hanke W and Sham L J 1980 *Phys. Rev.* B **21** 4656
[36] Kisiel A, Zimnal-Starnawska M, Antonangeli F, Piacentini M and Zema N 1986 *Nuovo Cimento* D **8** 436